

# 大規模歪に対応した Roll-to-Roll マスクレス露光装置の開発

堀 正和, 内藤一夫, 中野貴之, 伊倉良幸, 橋場成史, 鬼頭義昭

## Development of Roll-to-Roll Maskless Exposure System for Large-Scale Pattern Deformation

Masakazu HORI, Kazuo NAITO, Takayuki NAKANO, Yoshiyuki IGURA, Seiji HASHIBA and Yoshiaki KITO

フレキシブル基材の上に電子デバイスを作製したフレキシブルエレクトロニクスは、その柔軟性により従来のシリコンプロセスでは実現できなかった新しい機能が実現でき、多くの研究・応用がなされている。その製造技術として基材を連続的に処理する Roll-to-Roll 技術を用いると基材のハンドリング難易度が下がり歩留まり・生産性の向上が見込まれている。さらに Roll-to-Roll 技術は長さ方向のサイズ制限を受けず、長大なデバイスが生産できるため、鋭意研究・開発が進んでいる。

ところが、ポリマー材料を始めとするフレキシブル基板は従来のガラス、シリコン等と比較して熱的・機械安定性が格段に低く、電子デバイスの製造工程で従来と比較して100倍以上の大きな変形が生じることが分かっている。従来の露光装置ではこの大きな変形量を補正できず、フレキシブル基材上に電子デバイスを作製することは困難であった。

そこで、基材の変形量に対応できる補正ストロークの大きなマスクレス露光装置の開発を行った。この露光装置は基材の変形計測と露光を並列処理し連続的に露光が行える。開発した装置を使用して、A3サイズフィルムと Roll-to-Roll フィルムに対して露光評価を実施した。A3サイズ基板で実際のデバイス作製に近い条件において重ね合わせ $\pm 1.8 \mu\text{m}$ 、Roll-to-Roll 基板で重ね合わせ $\pm 4.0 \mu\text{m}$ の精度を達成したので詳細を報告する。

Flexible electronics, which is fabricated with electronic devices on flexible substrates, have been researched and applied, because of flexibility which was not realized in conventional silicon processes. By using Roll-to-Roll (R2R) technology, which continuously processes the substrate material, it is expected to reduce the difficulty of handling the substrate material and improve yield and productivity. In addition, R2R technology has merits for long-sized devices which is not subject to size restrictions in the length direction. However, flexible substrates such as polymer materials can be easily deformed during electronic device manufacturing process, like 100 times larger than conventional glass or silicon substrates, because of mechanical and thermal instability. It is difficult to fabricate electronic devices on flexible substrates with conventional exposure apparatuses, because they cannot compensate for large amount of deformation.

We have developed a maskless exposure system with a large correction stroke that can correspond to the amount of base material deformation. This exposure apparatus processes deformation measurement of the base material and exposure in parallel, and exposure is performed continuously. Exposure evaluation was performed for A3 size film and Roll-to-Roll film. We have achieved an overlay accuracy of  $\pm 1.8 \mu\text{m}$  for A3 size substrates and  $\pm 4.0 \mu\text{m}$  for R2R substrates, so we will report the details.

**Key words** 露光装置, マスクレス露光装置, フレキシブルエレクトロニクス, 重ね合わせ, ロールトゥロール exposure system, maskless exposure system, flexible electronics, overlay accuracy, roll-to-roll

## 1 Introduction

Conventional electronic devices rely on rigid substrates to host electronic components, whereas those assembled on soft substrates are considered flexible electronics. These devices are characterized by their lightweight, slim profile, flexibility, and stretchability, making them suitable for applications where traditional electronics would be unsuitable [1].

For instance, the adaptability of a substrate allows for bending, contraction, and excellent biocompatibility, enabling its integration as artificial skin to gather human body information [2]–[4]. Their lightweight nature and resistance to cracking also make them ideal for mobile and curved displays, leading to extensive research across various domains [5]–[7].

However, the thin and flexible nature of the polymer sub-

strate (“film substrate”) introduces handling challenges. An approach to address this issue is to fabricate the device using standard procedures, bonding it to a rigid substrate, and subsequently peeling it off [8]–[10]. However, this method necessitates an additional detachment step, and the stress incurred during both device fabrication and detachment is concentrated during the detachment process itself. Consequently, the design of a film configuration becomes crucial, thereby contributing to increased costs. An alternative solution under consideration involves the utilization of roll-to-roll transfer technology, a technique long employed in printing and other industries. This technology entails unwinding a substrate in a roll shape, guiding it using rollers, and rewinding it into a roll after processing. This approach allows for continuous handling of the substrate, preventing issues like wrinkling or buckling, thereby enhancing both productivity and yield. Moreover, the roll-to-roll process ensures the uninterrupted handling of the film, freeing the feeding direction of the film substrate from constraints posed by device size. This capability opens up the possibility of fabricating devices of unprecedented dimensions [11]–[13]. Numerous attempts have been made to fabricate devices on film substrates using roll-to-roll technology; however, these efforts have primarily focused on single-layer wiring procedures and the construction of expansive electrode structures. Examples of prototype electronic devices remain scarce. This is largely owing to film substrates exhibiting significantly lower thermal and mechanical stability compared to traditional materials like glass and silicon. Consequently, these substrates are prone to substantial deformation during the electronic device manufacturing process. Notably, conventional exposure devices cannot compensate for this large amount of deformation, making it difficult to fabricate electronic devices directly on the film substrate [14].

Therefore, to resolve this issue, we have successfully engineered a maskless exposure device capable of accommodating significant deformations in film substrates. Fig. 1 shows a photograph of the developed device. This exposure device is designed to enable roll-to-roll transfer of the film substrate, allowing for parallel processing of deformation and exposure measurements. Moreover, the device ensures continuous processing without necessitating to halt the transfer process.

However, creating patterns on the film substrate remains challenging. In this document, we delve into the technical challenges encountered during device development and present our proposed solutions. We then provide an over-

view of the developed device, detailing its exposure and alignment systems, along with the evaluation results. Finally, we discuss the outcomes of roll-to-roll exposure and showcase a sample device prototype produced using the newly developed maskless exposure device.



Fig. 1 Photograph of the developed direct drawing exposure device and transfer unit

## 2 Technical issues and solutions

To achieve precise exposure on flexible substrates, our device was developed based on the following key concepts:

### (1) Issues with film handling

Given their low mechanical strength, flexible films are susceptible to deformation owing to even minor changes in tension during transfer. Consequently, any external force applied to the film during the transition from alignment to exposure can lead to deformation, hindering the attainment of high-precision overlay exposure. Therefore, it is essential to maintain the film’s integrity and prevent deformation during the transfer process between alignment and exposure. In typical exposure devices, alignment and exposure are performed by securing the substrate onto a flat stage. However, when applied to thin and flexible films, this method can lead to significant deformations and wrinkles owing to surface adhesion. To overcome this challenge, we have adopted an alternative approach where the film is wrapped around a large roller, utilizing frictional force to secure it. The film is then transferred by rotating the roller. Upon initial contact with the roller, the film is fixed through line contact, effectively minimizing deformation. Alignment measurements are conducted directly on the roll’s surface, and exposure takes place in situ. To accommodate this configuration, all sensors are positioned along the roller’s curvature. Moreover, these rollers serve as a transfer mechanism, enabling continuous roll-to-roll processing of the film.

### (2) Issues with large film deformation

Film substrates exhibit deformations at a significantly higher rate of approximately 1000 ppm owing to heat and

film stress, which is 100 times greater than that of glass. Moreover, local stress is induced during pattern fabrication processes, resulting in nonlinear deformation specific to the pattern's shape. Hence, we opted for a maskless direct writing exposure technique capable of accommodating such deformations and substantial correction distances. Multiple options for maskless direct writing exposure methods are available. However, given the curved surface of the roller where exposure takes place, surface-based techniques are anticipated to result in the ends beyond the ridgeline of the roll falling out of the depth of focus. Therefore, we adopted a scanning method using polygons, enabling exposure along a one-dimensional straight line without relying on surface exposure.

### (3) Issues regarding productivity

The maskless exposure device operates by utilizing image data, where the device assesses film substrate deformations, digitally adjusts the original image, and subsequently performs exposure, allowing for substantial corrections. However, there is a time lag from measurement to image generation and development, posing a challenge for continuous processing. Furthermore, digital image corrections might cause quantization and misalignment issues, potentially disrupting wiring. While enhancing image resolution can alleviate quantization effects, it concurrently increases data size exponentially, thereby prolonging image processing. Thus, we adopted a technique that mechanically and optically transforms the exposure pattern while retaining the original exposure image data. Furthermore, a target exposure speed that can be feasibly attained in mass production is established. Details are given in the device description.

## 3 Details of developed device

### 3.1. Overview of overall device structure

Fig. 2 shows the overall structure of the developed roll-to-roll direct drawing exposure device.

The film is unwound from the roll, passes through the exposure unit, and is then rewound onto another roll. Both the unwinding and winding rolls are positioned on the same side, forming a U-shape transfer configuration that minimizes the device's overall length. A sensor measures the film's edge right after it leaves the roll, and the unwinding roll is adjusted to maintain a constant edge position relative to the device. This ensures a stable film position during exposure, reducing any potential deviations. The device can accommodate roll films up to 200 meters in length, assuming a film thickness of 100  $\mu\text{m}$ . Film substrates become charged

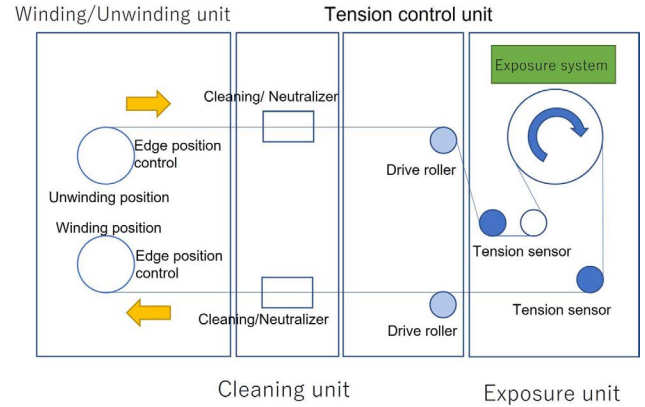


Fig. 2 Overview of overall exposure device configuration

by rubbing against the roll and peeling. A charged film destroys devices on the film and attracts particles in the air, causing defects. Therefore, we installed a unit that removes static electricity from the film and a cleaning unit that removes dust. The film substrate is a non-conductor and is transferred by multiple rollers; hence, the elimination of static electricity is particularly important.

The rotation speed of the roller within the exposure unit, referred to as the main roller, determines the transfer speed of the entire device. Maintaining a constant rotation speed for the main roller ensures the stability of the exposure position and the amount of exposure. Rollers with tension sensors attached in the front and backside of the main roller are installed, and the tension of the film introduced to the main roller is measured. Moreover, the tension of the film is controlled by the tension adjustment unit, which controls the difference in speed between the main roller and the drive roller and keeps the expansion and contraction of the film constant in the transfer direction.

The exposure system measures the alignment of the continuously transferred film in parallel and exposes it according to the position of the pattern measured by the alignment. Details of the exposure system are described below.

### 3.2. Exposure system

Fig. 3 shows a schematic of the developed exposure system. The exposure system was comprised of several components: an exposure module responsible for performing the exposure process, an alignment microscope used for measuring the film's shape, and an encoder read head along with an encoder ring, which were utilized to detect the precise position of the main roller. Components such as sensors were arranged along the curved surface of the main roller.

To increase the overall exposure width, we arranged six exposure modules into two rows with a staggered configuration. Each individual exposure module had a width of 50

mm, collectively providing a combined exposure area of 300 mm in width. Employing a direct writing exposure technique utilizing polygons, the exposure modules were capable of applying linear patterns, ensuring accurate exposure on curved rollers without encountering any defocusing problems.

The unit pixel size for direct exposure was set to  $2\ \mu\text{m}$  square. A total of seven alignment microscopes were placed at the joints of each module, facilitating alignment measurement over the entire exposure width.

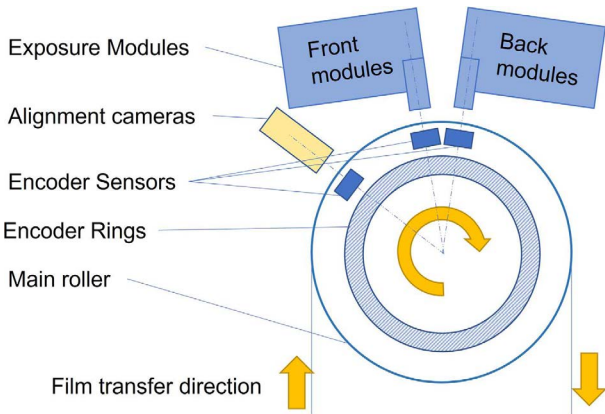


Fig. 3 Schematic side view of exposure system

Encoder rings were positioned on either side of the main roller to monitor its rotation. The encoder heads were aligned in two rows corresponding to the arrangement of the exposure module, ensuring adherence to Abbe’s principle and minimizing measurement inaccuracies. Employing a three-phase design, each encoder head utilized the shared Z-phase on the encoder ring to establish calibration origins for each encoder. Please refer to Fig. 4, an expansion of Fig. 3 on a plane, for visual reference.

When employing the direct drawing exposure technique with a polygon mirror, exposure is hindered when the exposure light encounters the corners of the polygon mirror. This limitation prevents the polygon mirror from being utilized to its full extent. Fig. 5 shows a schematic diagram of the usable angle of the polygon and the exposure timing chart. In the example below, if only one-third of the octagonal polygon’s surface area can be allocated for exposure, the efficiency of light source utilization becomes limited to one-third. To enhance the efficiency of light source utilization, a time-division method is employed, whereby the light source is shared among the three polygons. This is achieved by shifting the phase of each polygon by 15 degrees to ensure that their exposure angles do not align temporally. Consequently, one polygon is consistently in the exposed state, resulting in nearly 100% light source utilization efficiency and

enhanced productivity.

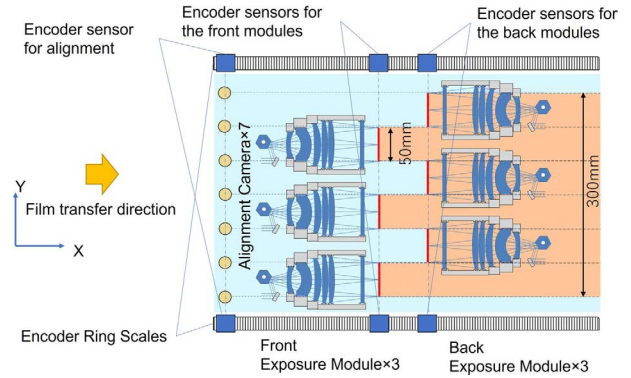


Fig. 4 Schematic diagram of exposure system development

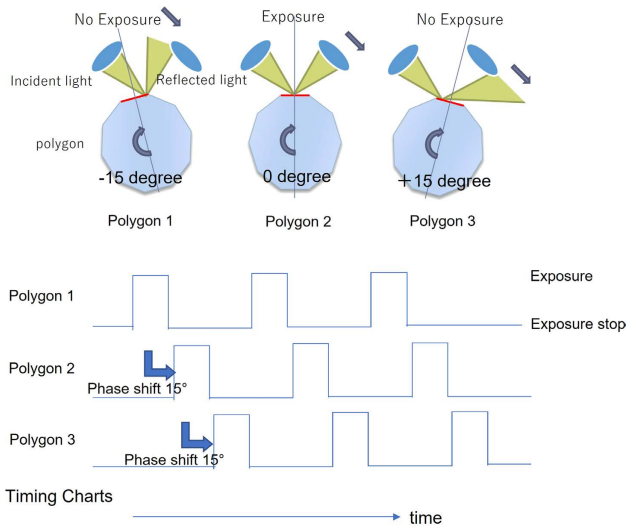


Fig. 5 Highly efficient utilization of polygons

### 3.3. Exposure results

Fig. 6 displays an image of the resolution chart that was exposed using the developed exposure system. The procedure involved applying a  $1\text{-}\mu\text{m}$  layer of photoresist OFPR-5000LB (Tokyo Ohka Kogyo Co., Ltd., Kanagawa, Japan) onto a poly ethylene terephthalate (PET) film, which was further coated with a 100-nm layer of vapor-deposited Cu. Subsequently, exposure took place. Following exposure, the film was subjected to one-minute development using a 2.38% concentration of tetramethylammonium hydroxide (TMAH). Notably, the exposure process was based on the bit-map image (BMP) format image data stored in the device, and that each module achieved a minimum resolution of  $4\ \mu\text{m}$  line/space (L/S). The results confirmed that practical patterns, with an L/S of  $6\ \mu\text{m}$ , could effectively be generated within a 300 mm width using arbitrary image data.

### 3.4. Exposure pattern deformation method

The newly developed exposure device facilitates a real-

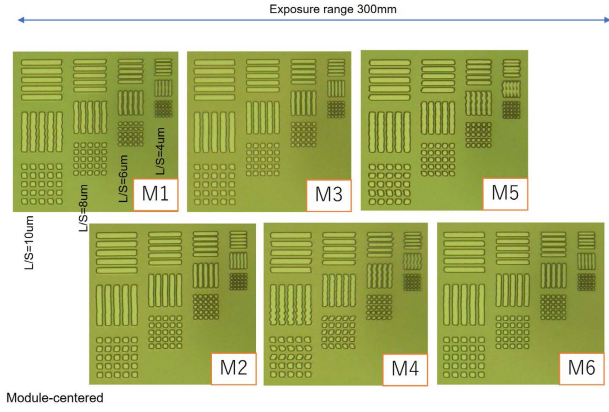


Fig. 6 Resolution chart pattern exposure result

time transformation of the exposure pattern by altering the drawing position optically and mechanically while preserving the original exposure image data. This is achieved by dynamically adjusting the exposure lines scanned by the polygon mirror within the regions delimited by each of the six exposure modules. This real-time correction addresses intricate and substantial deformations effectively. As shown in Fig. 7, there are four components to be changed (shift Y/Y magnification/X magnification/rotation). The deformation method for each component is described below.

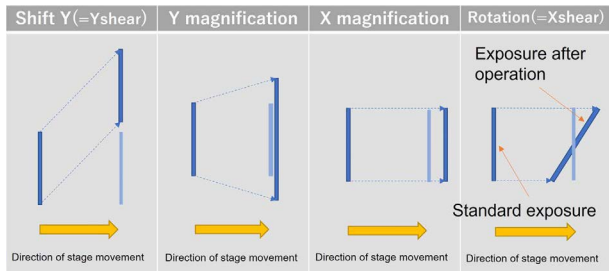


Fig. 7 Diagram of each correction operation

### 3.4.1. Shift Y (=Y shear)

The Y direction corresponds to the polygon scanning direction. Shifting the exposure position in the Y direction involves introducing a time offset to the polygon scan initiation time. The combination of roller rotation and the Y shift operation permits the induction of Y shear deformation. The vector diagram of the exposure outcomes with continuous Y shift alterations is shown in Fig. 8(a).

### 3.4.2. Y Magnification

Y magnification induces slight alterations in the exposure interval by modifying the light emission cycle of the light source, resulting in overall scaling changes. The periodic modulation can be adjusted for each polygon face, enabling exposure while smoothly varying the magnification. Fig. 8(b) portrays a vector diagram illustrating the outcomes of continuous Y magnification adjustments.

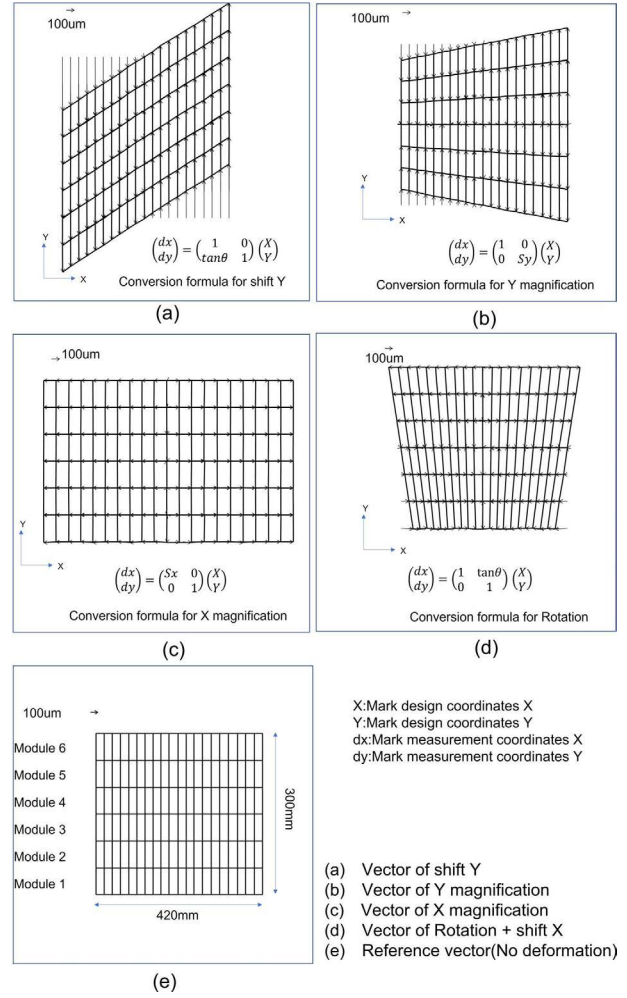


Fig. 8 Vector diagram of pattern deformation exposure result

### 3.4.3. X Magnification

The X direction corresponds to the roller rotation direction. The X magnification is altered by adjusting the correlation between the roller and rotation speeds of the polygon mirror. For instance, if the stage maintains a constant speed, elevating the polygon's rotation speed heightens the exposure density, resulting in pattern contraction. Conversely, decreasing the rotation speed elongates the Y pattern. Fig. 8(c) shows a vector diagram illustrating the outcomes of implementing adjustments to X magnification.

### 3.4.4. Rotation (= X shear)/Shift X

The device incorporates a mechanism capable of mechanically rotating the module around its center, using the 50 mm exposure range of the module as a pivot reference. This rotational capability allows for the manipulation of the exposure pattern. When combined with the roller-driven film transfer motion, this mechanism facilitates deformation in the X shear direction. Furthermore, each module is furnished with an optical element that introduces an exposure position shift along the X axis. Activating this element during exposure enables individualized shift adjustments (X-shift)

for each module. In Fig. 8(d), the vector diagram illustrates the results obtained from continuous module rotation. Although the amount of rotation is consistent for each module, the integration of rotation with an X-shift introduces a transformation of the trapezoidal shape.

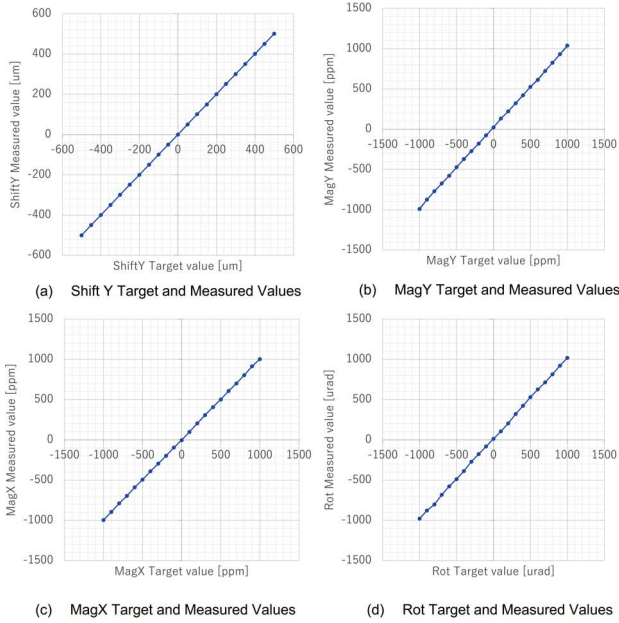


Fig. 9 Relationship between the exposure indication and measured values

Fig. 9 shows the linearity measurement results corresponding to each deformation motion shown in Fig. 8. The X axis shows the exposure machine target value, whereas the Y axis shows the actually measured deformation amount. Fig. 9(a) demonstrates the linear operation within the scope of  $-500 \mu\text{m}$  to  $500 \mu\text{m}$  for shift Y. In Fig. 9(b), the Y magnification operates linearly between  $-1000 \text{ ppm}$  and  $1000 \text{ ppm}$ . Similarly, Fig. 9(c) showcases the linear operation of X magnification within a range of  $-1000 \text{ ppm}$  to  $1000 \text{ ppm}$ . Finally, Fig. 9(d) portrays the linear behavior of rotation, ranging from  $-1000 \mu\text{rad}$  to  $1000 \mu\text{rad}$ .

## 4 Overlay exposure

The alignment measurement process of the developed device is outlined as follows. The film's X-direction position is measured by taking measurements synchronized with the encoder's position during the film's transfer. Aligned along the Y direction, the alignment microscope measures the film's Y-direction position. The magnitude of film deformation can be ascertained by comparing the alignment microscope's measured mark position with its designated value. Although this procedure is performed within each module, the alignment camera is shared among neighboring mod-

ules. This arrangement enables seamless calculations across modules, maintaining pattern consistency even in cases where exposure module joints or alignment rows are switched.

Following the computation of correction values for each pattern deformation component from the alignment measurements, the exposure unit then proceeds to conduct exposure based on these correction values. Fig. 10 shows the alignment calculation model. The correction amount is calculated using the model formula from the measurement results of the alignment microscope and the design coordinates. Continuous patterns such as the roll-to-roll case are handled by repeating this calculation for each column.

### 4.1. Overlay accuracy evaluation and results

The results of evaluating the alignment measurement and overlay exposure are described. The results of fabricating a laminated structure on an A3-sized film and the results of fabricating a laminated structure by transferring the film by a roll-to-roll method are shown.

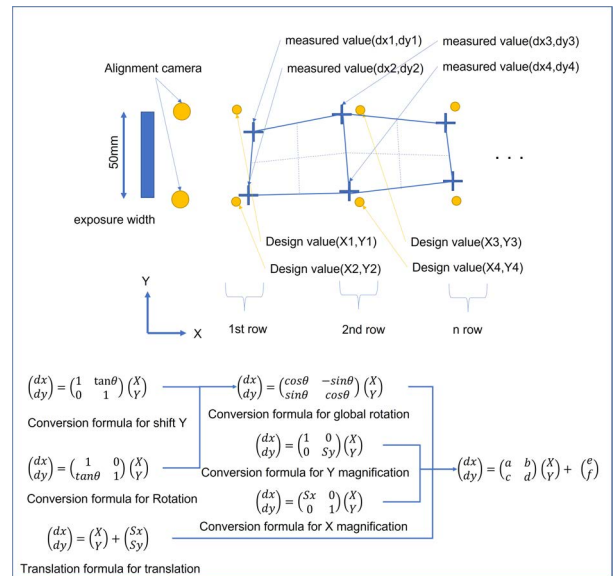


Fig. 10 Alignment calculation model

#### 4.1.1. Evaluation results for A3 size film

A multilayer structure consisting of Al/SiO<sub>2</sub>/Al/protective film was fabricated on an A3-size PI film. Photolithography was used to process metal wiring and open patterns on each layer. Additionally, an intermediate layer was annealed at 200 °C for one hour. Fig. 11(a) shows the vector diagram of the shape of the film when processing the protective film, and Fig. 11(b) shows the vector diagram of the measurement error amount when conducting overlay exposure.

The film's shape in Fig. 11(a) exhibits contraction along the longitudinal and expansion along the lateral direction due

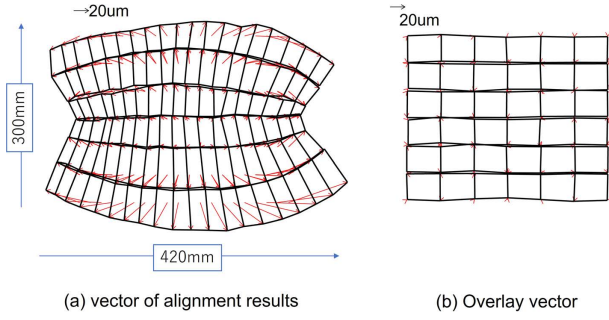


Fig. 11 Evaluation result of overlay accuracy on A3 film

to film stress and annealing. Achieving overlay exposure on such a shape using conventional exposure devices is challenging. However, the exposure device developed in this context demonstrates the capability to perform exposure while accommodating the film's deformation. Fig. 12 shows the histogram of the overlay error amount of the exposed film. The overlay accuracy has a mean of  $+3\sigma$  and is  $\pm 1.8 \mu\text{m}$  for both X and Y. Furthermore, the device was verified to successfully track the film's deformation and execute overlay exposure for all other layers.

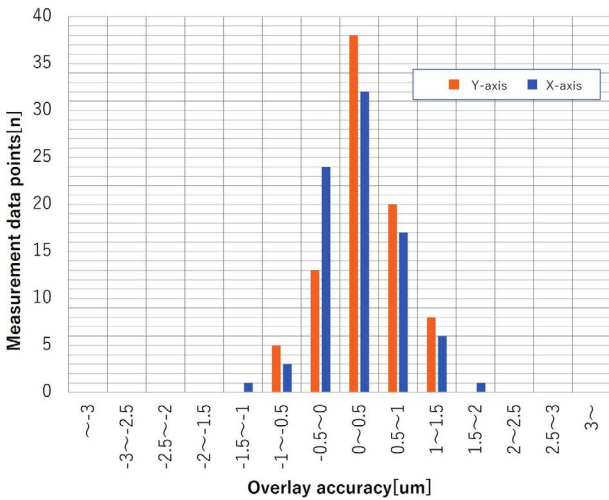


Fig. 12 Histogram of A3 film overlay error amount

#### 4.1.2. Roll-to-roll evaluation results

After continuously forming Al wiring for 20 m using the roll-to-roll method, an insulating layer was formed and annealed. An aperture pattern was formed by photolithography while aligning the film in this state. Fig. 13 shows the film shape and measurement results of overlay exposure when alignment exposure was conducted on the film.

The alignment results indicate elongation in the X direction and a meandering component in the Y direction. Moreover, deformation is possibly caused by the process. However, the overlay outcomes have been adequately rectified, and the histogram presented in Fig. 14 demonstrates that the overlay accuracy remains within a range of  $\pm 4 \mu\text{m}$ . In a

previous report, we presented the findings of film patterning, confirming the successful fabrication of highly precise long-distance patterning under conditions that closely resemble actual processing [15].

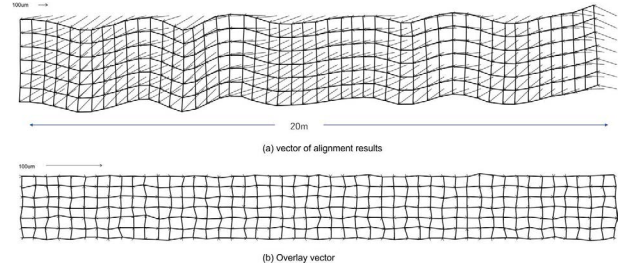


Fig. 13 Overlay accuracy evaluation results during roll-to-roll exposure

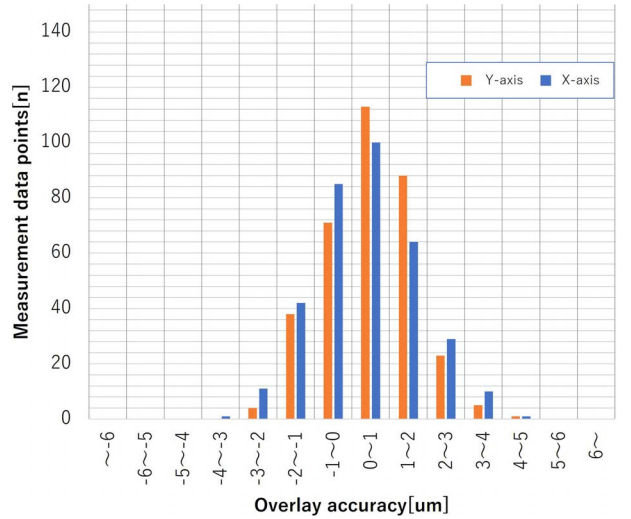


Fig. 14 Histogram of roll-to-roll overlay error amount

## 5 Pattern fabrication example

We have successfully validated the feasibility of generating a wide range of patterns on films using the exposure device, encompassing laminated structures and monolayer wiring patterns. In Fig. 15, we illustrate an actual prototype of an extended pattern. Our efforts have extended beyond refining the exposure process; we have also designed equipment that supports the roll-to-roll process, enabling the creation of continuous patterns spanning at least 20 meters in all roll-to-roll procedures. During the device prototyping phase, iterative checks and adjustments are typically necessary in each process, impacting patterns. However, given that this device operates as a maskless direct drawing exposure system, adjustments can be seamlessly implemented by altering the computer aided design (CAD) data, leading to an enhanced prototyping cycle and increased frequency of trials. Moreover, when producing devices that harness flexible proper-



Fig. 15 Prototyped long pattern



(a)



(b)

**Artist** Katsushika Hokusai  
**Title** Under the Wave off Kanagawa, also known as The Great Wave, from the series Thirty-Six Views of Mount Fuji (Fugaku sanjūrokkei)  
**Place** Japan (Object made in)  
**Date** 1826–1836  
 The Art Institute of Chicago

Fig. 16 Thirty-Six Views of Mt. Fuji exposed by maskless exposure machine

ties, such as flexible electronics, precision in shaping the devices to match their intended form and function is crucial. With a maskless approach, the potential for on-demand manufacturing emerges, allowing for tailored fabrication based on specific applications through image data updates. This flexibility also enables the prototyping of devices with diverse shapes within an extended film. To illustrate this capability, Fig. 16 presents an exposure demonstration of an arbitrary pattern derived from the image “Thirty-Six Views of Mt. Fuji”. In Fig. 16(b), the original image is depicted, whereas Fig. 16(a) demonstrates the exposed image with dimensions of  $800\ \mu\text{m} \times 600\ \mu\text{m}$ . Notably, a highly intricate pattern has been achieved, even capturing subtle details such as water splashes in miniature regions.

## 6 Conclusion

In summary, our development of a maskless exposure device capable of achieving high-precision overlay exposure on films with significant deformation achieved promising results. We successfully demonstrated the creation of laminated films requiring precise alignment, ranging from A3-sized films to continuous films extending over 20 meters. Notably, for A3-sized films, we verified the attainment of sub- $2\ \mu\text{m}$  accuracy for overlaying patterns as fine as  $6\ \mu\text{m}$  L/S (Line/Space) on extensively deformed films subjected to deposition and annealing processes.

An additional advantage lies in the adaptability of the exposure pattern through simple modifications of CAD data. This capability proved highly valuable for rapid prototyping and the realization of on-demand patterns. Moreover, the exposure device holds particular promise for the roll-to-roll method, enabling the flexible production of a diverse array of electronic devices. We anticipate that our device will significantly contribute to the advancement of flexible electronics.

## References

- [1] K. Kuribara *et al.* “Organic transistors with high thermal stability for medical applications,” *Nature Communications*, Vol. 3, 723, 2012.
- [2] B. Wang *et al.* “Foundry-compatible high-resolution patterning of vertically phase-separated semiconducting films for ultraflexible organic electronics,” *Nature Communications*, Vol. 12, 4937, 2021.
- [3] M. Kaltenbrunner *et al.* “Ultrathin, highly flexible and stretchable PLEDs,” *Nature Photonics*, Vol. 7, pp. 811–816, 2013.
- [4] K. Nomura, H. Ohta, A. Takagi, T. Kamiya, M. Hirano and

- H. Hosono, "Room-temperature fabrication of transparent flexible thin-film transistors using amorphous oxide semiconductors," *Nature*, Vol. 432, pp. 488-492, 2004.
- [6] L. Zhou, A. Wang, S. Wu, J. Sun, S. Park and T. N. Jackson, "All-organic Active Matrix Flexible Display," *Appl. Phys. Lett.*, Vol. 88, 083502, 2006.
- [7] I. Yagi *et al.* "A Full-Color, Top-Emission AM-OLED Display Driven," *SID 07 DIGEST*, Vol. 63-2, pp. 1753-1757, 2007.
- [8] M. Mizukami *et al.* "Flexible AM OLED Panel Driven by Bottom-contact OTFTs," *IEEE Electron. Dev. Lett.*, Vol. 27, pp. 249-251, 2006.
- [9] Y. Nakajima *et al.* "Improvement in Image Quality of a 5.8-in. OTFT-Driven Flexible AMOLED Display," *Journal of the SID*, Vol. 19, pp. 94-99, 2011.
- [10] M. Nakata *et al.* "Development of Flexible Displays Using Back-channel-etched In-Sn-Zn-O Thin-film Transistors and Air-stable Inverted Organic Light-emitting Diodes," *Journal of the SID*, Vol. 24-1, pp. 3-11, 2016.
- [11] T. Aoyama *et al.* "An 8.34-inch 1058-ppi 8K x 4K Flexible OLED Display," *SID 2017 DIGEST*, Vol. 24-3, pp. 338-341, 2017.
- [12] J. Yoon *et al.* "World 1st Large Size 18-inch Flexible OLED Display and the Key Technologies," *SID 2015 DIGEST*, Vol. 65-1, pp. 962-965, 2015.
- [13] J. Hong *et al.* "The First 9.1-inch Stretchable AMOLED Display Based on LTPS Technology," *SID 2017 DIGEST*, Vol. 5-5, pp. 47-50, 2017.
- [14] H. Shin *et al.* "Advanced OLED Display Technologies for Large-Size Semi-Flexible TVs," *SID 2017 DIGEST*, Vol. 45-2, pp. 609-612, 2016.
- [15] Y. Kito *et al.* "Direct Imaging Exposure Equipment with High Overlay Accuracy for Flexible Substrate in Roll-to-Roll Method," *Proceeding of IDW 16*, pp. 515-518, 2016.
- [16] Y. Kito *et al.* "Novel Direct Imaging Exposure System with High Productivity for Flexible Substrate in Roll-to-Roll Method," *Proceeding of IDW 17*, pp. 500-512, 2017.

堀 正和 Masakazu HORI  
 FPD 装置事業部開発統括部 先端技術開発部  
 Advanced Technology Development Department  
 Development Sector, FPD Lithography Business Unit

内藤一夫 Kazuo NAITO  
 FPD 装置事業部開発統括部 先端技術開発部  
 Advanced Technology Development Department  
 Development Sector, FPD Lithography Business Unit

中野貴之 Takayuki NAKANO  
 FPD 装置事業部開発統括部 先端技術開発部  
 Advanced Technology Development Department  
 Development Sector, FPD Lithography Business Unit

伊倉良幸 Yoshiyuki IGURA  
 FPD 装置事業部開発統括部 先端技術開発部  
 Advanced Technology Development Department  
 Development Sector, FPD Lithography Business Unit

橋場成史 Seiji HASHIBA  
 FPD 装置事業部開発統括部 先端技術開発部  
 Advanced Technology Development Department  
 Development Sector, FPD Lithography Business Unit

鬼頭義昭 Yoshiaki KITO  
 FPD 装置事業部開発統括部 先端技術開発部  
 Advanced Technology Development Department  
 Development Sector, FPD Lithography Business Unit